

Biomechanics of Skull Fracture

NARAYAN YOGANANDAN,¹ FRANK A. PINTAR,¹ ANTHONY SANCES, JR.,¹
PATRICK R. WALSH,¹ CHANNING L. EWING,²
DANIEL J. THOMAS,³ and RICHARD G. SNYDER⁴

ABSTRACT

This study was conducted to determine the biomechanics of the human head under quasistatic and dynamic loads. Twelve unembalmed intact human cadaver heads were tested to failure using an electrohydraulic testing device. Quasistatic loading was done at a rate of 2.5 mm/s. Impact loading tests were conducted at a rate of 7.1 to 8.0 m/s. Vertex, parietal, temporal, frontal, and occipital regions were selected as the loading sites. Pathological alterations were determined by pretest and posttest radiography, close-up computed tomography (CT) images, macroscopic evaluation, and defleshing techniques. Biomechanical force-deflection response, stiffness, and energy-absorbing characteristics were obtained. Results indicated the skull to have nonlinear structural response. The failure loads, deflections, stiffness, and energies ranged from 4.5 to 14.1 kN, 3.4 to 16.6 mm, 467 to 5867 N/mm, and 14.1 to 68.5 J, respectively. The overall mean values of these parameters for quasistatic and dynamic loads were 6.4 kN (± 1.1), 12.0 mm (± 1.6), 812 N/mm (± 139), 33.5 J (± 8.5), and 11.9 kN (± 0.9), 5.8 mm (± 1.0), 4023 N/mm (± 541), 28.0 J (± 5.1), respectively. It should be emphasized that these values do not account for the individual variations in the anatomical locations on the cranium of the specimens. While the X-rays and CT scans identified the fracture, the precise direction and location of the impact on the skull were not apparent in these images. Fracture widths were consistently wider at sites remote from the loading region. Consequently, based on retrospective images, it may not be appropriate to extrapolate the anatomical region that sustained the impact forces. The quantified biomechanical response parameters will assist in the development and validation of finite element models of head injury.

Key words: biomechanics; dynamic loading; human tolerance; impact response; skull fracture; static loading

INTRODUCTION

HHEAD INJURIES have significant impact on our society. Not only are the economic costs staggering, but also the quality of life of the individual is affected.

Consequently, research efforts to determine the cause, the epidemiology, and the intervention measures to ameliorate this problem are of critical importance. From the causal standpoint, head injuries often result from dynamic forces applied to the calvarium and transmitted to the

¹Department of Neurosurgery, Medical College of Wisconsin, and Veterans Affairs Medical Center, Milwaukee, Wisconsin.

²Ewing Biodynamics Corporation, New Orleans, Louisiana.

³Hoechst Celanese Corporation, Somerville, New Jersey.

⁴BioDynamics International, Tucson, Arizona.

brain. Depending on the nature and extent of the dynamic force, and the individual demographics, different types of head injuries can occur. Primarily, head injuries are classified as open and closed. In the open type, the skull is penetrated and the intracranial contents may or may not show damage. In contrast, in the closed type, the skull is not fractured but the internal contents exhibit certain abnormalities. Diffuse axonal injury is an example of closed head injury. From an epidemiological standpoint, there exists considerable evidence in literature regarding impact loading of the human head with the vehicular component (e.g., A-Pillar) in motor vehicle accidents (Dimasi et al., 1991; Ewing et al., 1983; Harris et al., 1981; Sances et al., 1981; Sances and Yoganandan, 1986). Reviews of head injury literature are also available (Ewing et al., 1983; McElhaney et al., 1972; Melvin et al., 1993; Sances et al., 1981; Sances and Yoganandan, 1986; Snyder, 1970).

To understand the mechanisms of injury, develop tolerance criteria, provide fundamental data to mathematical analogues such as the finite element model for its validation, parametric studies, and injury prediction, and design anthropomorphic tests devices, it is important to conduct controlled laboratory studies using appropriate models of head injury. Physical models provide good control over the experiment, however, the mechanisms of injury cannot be delineated. Animal models provide an opportunity to monitor the physiologic response, however, other constraints including the scaling to the living human limit their applicability. Human cadaver experiments, despite the postmortem characteristics of the tissue, offer a unique opportunity to understand certain aspects of head injuries. Because of the anatomical similarities with the living human, it may be appropriate to extrapolate to real-world situations.

As indicated earlier, the two basic constituents of the

head are the calvarium and its intracranial contents, i.e., brain matter. To investigate the biomechanical aspects of head injury, it is imperative to understand the behavior of both components. In addition, impact forces applied to the head result in deformations of the skull producing fracture, i.e., open head injury. Depending on the anatomical site where the impact blow is delivered, varying degrees of pathology are possible. Consequently, it is important to delineate the biomechanics of skull fracture and determine the associated bioengineering variables such as forces, deformations, stiffness, and energies, and correlate the trauma with these parameters. The present investigation was conducted to delineate the biomechanics of skull fracture secondary to quasistatic and dynamic external loading to the various regions of the skull.

MATERIALS AND METHODS

Specimen Preparation and Mounting

Unembalmed human cadavers were used in the study. The age, height, and weight ranged from 50 to 76 years, 1.6 to 1.8 m, and 50 to 102 kg, respectively. There were five males and seven females (Table 1). The selection was based on preradiography and medical records to exclude subjects with severe degenerative or bone disease. The specimens were isolated at the OC-C1-C2 junction keeping the intracranial contents intact. Pretest X-rays and computed tomography (CT) images were obtained at 1.0 to 1.5 mm intervals using a CT scanner (Model: High Speed Advantage, General Electric Medical Systems, Waukesha, WI). Physical measurements such as the nasion-occiput distance and the maximum circumference of the head were obtained. Table 2 includes the data for each specimen along with the mean values of the para-

TABLE 1. SPECIMEN DATA^a

<i>ID</i>	<i>Sex</i>	<i>Age</i>	<i>Ht (cm)</i>	<i>Wt (kg)</i>	<i>Impact site</i>
1	M	65	173	50	Vertex
2	M	75	185	68	45° right lateral
3	F	63	168	77	45° right lateral
4	F	76	157	102	78° right lateral
5	M	70	183	86	45° frontal
6	F	74	165	73	45° rear
7	M	65	185	95	Vertex
8	F	67	165	68	45° frontal
9	F	50	168	84	Vertex
10	F	61	162	61	35° rear
11	M	—	—	—	Vertex
12	F	78	160	36	Vertex

^aSee Figure 2 for the schematic of the anatomical location on the specimen.

BIOMECHANICS OF SKULL FRACTURE

TABLE 2. PHYSICAL DATA

ID	<i>Lateral-lateral</i> (cm)	<i>Anteroposterior</i> (cm)	<i>Nasion-occiput</i> (cm)	<i>Inferior-superior</i> (cm)	<i>Circumference</i> (cm)	<i>Skin thickness at impact site</i> (cm)	<i>Weight</i> (kg)
1	15.2	20.0	19.4	15.9	58.4	0.6	3.98
2	15.9	19.1	18.7	16.2	61.0	0.9	4.09
3	16.2	20.0	19.8	16.2	57.2	0.8	4.29
4	14.3	18.6	18.4	13.5	54.9	0.7	3.21
5	16.2	19.7	19.1	15.6	59.4	0.7	4.72
6	14.6	18.7	16.5	16.2	52.7	0.6	—
7	15.6	18.7	21.6	16.8	57.8	0.8	4.12
8	14.0	19.1	17.5	15.9	54.6	0.5	3.21
9	15.9	18.1	17.5	15.9	57.2	1.0	3.41
10	14.0	18.4	17.1	14.9	54.0	0.8	3.34
11	14.6	19.1	19.4	14.3	54.6	0.5	3.52
12	14.7	16.5	17.0	14.5	49.5	0.5	2.81
Mean	15.1	18.8	18.5	15.5	55.9	0.7	3.70
SE	(± 0.2)	(± 0.3)	(± 0.4)	(± 0.3)	(± 0.9)	(± 0.1)	(± 0.17)

eters. The specimens were prepared with a fixation device to achieve rigid boundary conditions at the distal end. A jig was designed for this purpose. It consisted of a rigid platform onto which a U-shaped heavy-duty bracket was mounted. The jig was used to rigidly fix the screws into the auditory meatii of the specimen. This fixation device permitted the preparation to receive direct contact, static or dynamic loads at the following anatomical sites: vertex, parietal, temporal, frontal, and occiput. Figure 1 illustrates the fixation device along with the right-handed Cartesian coordinate system in accordance with the ISO Standards; Figure 2 includes a schematic of the five loading sites on the specimen showing the orientation and the force vector.

Loading Procedure

Following initial radiography, the specimens were oriented such that the desired site of loading was aligned appropriately with the vertical axis of the testing actuator. The specimen along with the fixation device was positioned on an electrohydraulic testing device (MTS Corporation, Minneapolis, MN) via an x-y cross table and a load cell (Denton, Inc., Rochester Hills, MI) to record the generalized force histories. The specimens were loaded once to failure at quasistatic or at dynamic rates. A hemispherical anvil with a radius of 48 mm was the loading surface used in the study. The anvil was rigidly attached to the electrohydraulic actuator. All quasistatic experiments were conducted at a loading rate of 2.54 mm/s. Failure was identified as the level at which a further increase in piston excursion resulted in a decrease

of the force. Dynamic tests were conducted by applying the load through the piston at velocities ranging from 7.1 to 8.0 m/s and the piston excursion was set at a predetermined limit. The piston impacted the cranium at a constant velocity. After the test, the specimen was palpated,

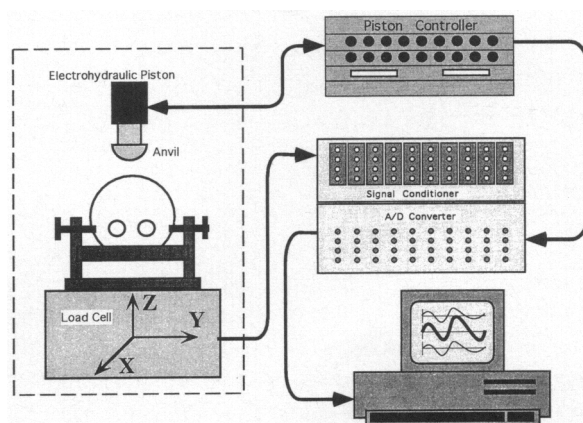


FIG. 1. Experimental setup indicating the custom-designed fixation device capable of orienting the specimen at a desired location, the distal load cell, the electrohydraulic piston for applying controlled quasistatic and dynamic loads, the piston controller housing the function generator for the testing device, the signal conditioning equipment, analog to digital (A/D) converter, and the computer used to acquire biomechanical data. The right-handed Cartesian coordinate system of reference with the z-axis oriented along the vertical direction is also shown. This is in accordance with the ISO coordinate system.

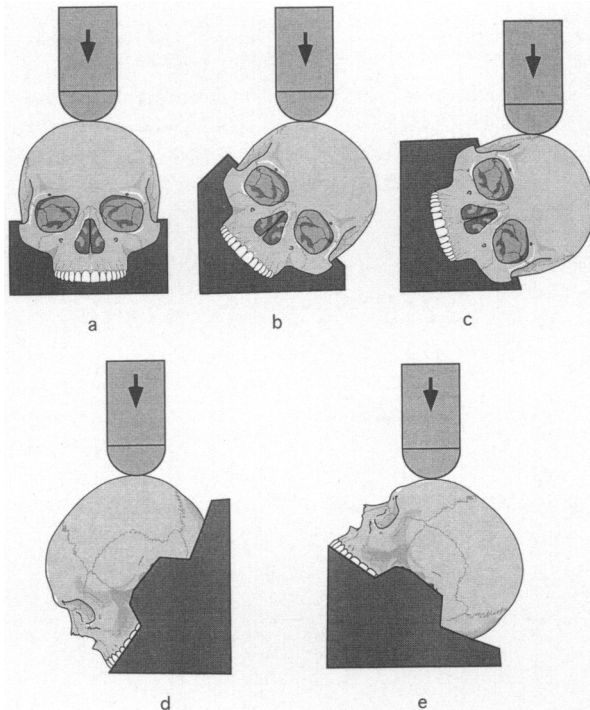


FIG. 2. Schematics of the specimen orientation in the fixation device and the external load (shown by dark arrow) applied by the electrohydraulic piston. (a) Vertex, (b) 45° right lateral (parietal), (c) 78° right lateral (temporal), (d) 45° rearward (occipital), and (e) 45° forward (frontal) regions.

macroscopically examined and radiographed for pathology. Computed tomography sections were obtained according to procedures described earlier. The specimen was defleshed.

Biomechanical Data

Applied external force and the actuator displacement were recorded with a uniaxial force gauge and a linear variable differential transformer attached in series with the electrohydraulic piston. In addition, the output force histories were recorded with the distal load cell. Data were gathered with a modular digital data acquisition system (Kaye Instruments, Boston, MA). Dynamic tests data were sampled according to the Society of Automotive Engineers SAE J211b specifications at a frequency of 8000 Hz. Figure 1 includes the schematic of the loading, the preparation, and the signal conditioning apparatuses used to acquire and process the data. A four-channel digital oscilloscope (Gould Instruments, London, England) was used to supplement the system. Biomechanical data processing included the transformation of the force–time and deflection–time signals to a force–deformation response. The output force–deforma-

tion response was then used to compute the stiffness and energy absorbing characteristics of the structure. Stiffness of the structure was defined as the slope of the force–deflection response in the linear-most region of the force–deflection behavior. The energy absorbing capacity was defined as the integral or the area under the force–deflection curve. In addition to the stiffness and energy absorption parameters, the ultimate force and the corresponding deflection were obtained.

RESULTS

Force–deflection biomechanical responses indicated nonlinear characteristics, typical of biological materials reported in literature (Yoganandan et al., 1989). Representative force–deflection responses from quasistatic and dynamic tests loaded at the vertex are included in Figure 3A. Failure forces and displacements ranged from 4.5 to 11.9 kN and 7.8 to 16.6 mm for the quasistatic tests, and from 8.8 kN to 14.1 kN and 3.4 to 9.8 mm for the dynamic tests, respectively. Table 3 includes the data for each specimen as well as the associated statistical parameters. The data from all the specimens for quasistatic and dynamic cases, without regard to the anatomical locations, are presented in the form of one plot each (Fig. 3B and C).

The off-axis forces recorded by the distal load cell were significantly lower compared to the peak input force with the exception of one specimen. The off-axis forces, i.e., F_y and F_x (Fig. 1), indicate the components of the force in two mutually orthogonal directions with the external loading applied in the vertical direction. In other words, these forces represent the unintended components sustained by the specimen. Since the magnitudes of these forces were within 10% of the peak magnitude of the applied force vector (F_z), the specimens can be considered to have sustained predominantly only the intended insult (Fig. 3D). In fact, this established procedure to ensure the purity of the loading vector has been used in other *in vitro* biomechanical studies (Yoganandan et al., 1995).

The stiffness of the structure ranged from 467 to 1290 N/mm for quasistatic loading and from 2462 to 5867 N/mm for dynamic loading tests (Table 3). The energy absorbing capacities ranged from 14.1 to 68.5 J for the quasistatic and from 14.1 to 43.5 J for the dynamic experiments. The pathology included linear and circular fractures, propagated unilateral and bilateral fractures, and multiple fractures due to external loading. Table 3 includes a brief summary of the pathology sustained by each specimen. Routinely, fractures identified on CT images were documented by the defleshed skull.

BIOMECHANICS OF SKULL FRACTURE

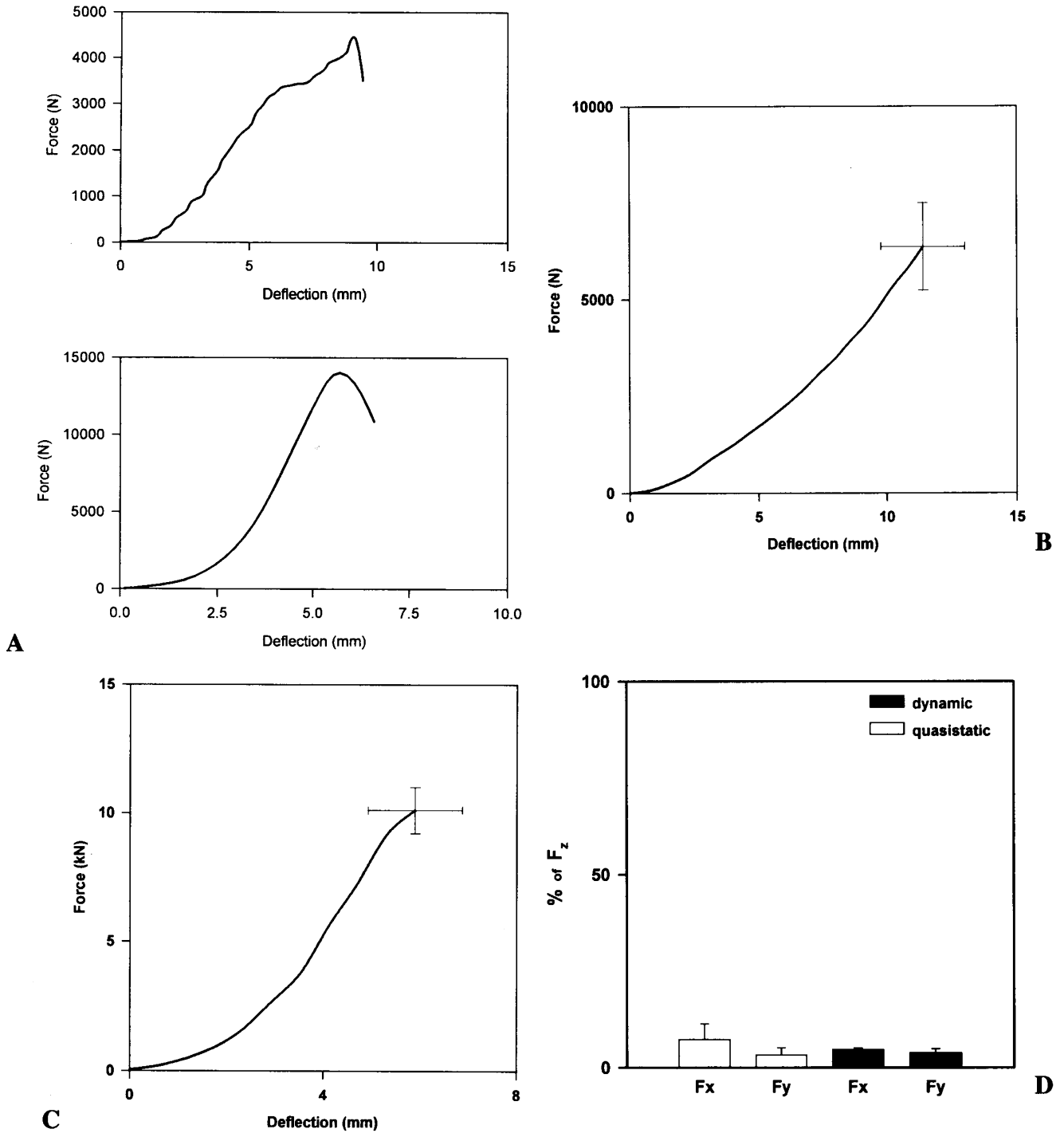


FIG. 3. (A) Top: force–deflection response of specimen (#1) tested quasistatically at the vertex. Bottom: response of specimen (#7) loaded dynamically at 7.2 m/s at the vertex. (B) Force–deflection responses for quasistatic tests. These data are independent of the loading site. (C) Force–deflection response for dynamic tests. These data are independent of the loading site. (D) Relative contribution of the off-axis forces in the quasistatic and dynamic experiments as a percentage of the peak applied vertical force.

DISCUSSION

As stated in the Introduction, head injuries result from an application of the impact force to the cranium. Fractures occur when the dynamic input exceeds the tolerance of the skull. In the present study, to understand the biomechanics, both quasistatic and dynamic experiments were conducted. The quasistatic tests provided the fundamental biomechanical data. It also facilitated designing an appropriate methodology so that the preparation could be mounted to a fixation device that permitted the alignment of the cadaveric specimen to accept the external loading. Furthermore, the quasistatic experiments, being relatively easy to conduct, provide a basis for comparative evaluation of the dynamic data.

These tests revealed the fracture pattern to be complex and dependent on the anatomical location of the loading site. Routinely, examination of the X-ray and CT images failed to reveal the precise direction and location of the impact site to produce the pathology. In fact, fracture widths were narrower at the loading site compared to the other regions where the specimen demonstrated wider separations of the fracture lines. This observation was vivid from the defleshed skulls and observed for both

quasistatic and dynamic tests. For example, CT images of specimen #7 impacted at the vertex, showed no damage at the loading site (Fig. 4A), while the caudal scans indicated fractures of the frontal bone (Fig. 4B) and fractures of the frontal sinus (Fig. 4C). The defleshed skull indicated more widening of these fractures at sites remote from the vertex (Fig. 4D). In an earlier study, Gurdjian reported similar findings using the stress coat technique and impacting (using the drop method) intact and dry human skulls onto a flat steel slab placed on a terrazzo cement floor (Gurdjian and Webster, 1958). Single linear fractures reported in this previous study matched with our experiments conducted using the electrohydraulic loading device. Although the Gurdjian study reported the fracture pathology and the impact energy (computed as the product of weight and the height), force-deflection responses of the skull were not reported. From this point of view, a comparison of the continuously quantified biomechanical parameters is not possible.

In quasistatic loading experiments, fractures of the inner and outer table consistently occurred; the force-deflection curves in certain cases demonstrated multiple peaks. For example, Figure 3 shows an early peak at a force of 3.4 kN at a corresponding displacement of 6.9

TABLE 3. BIOMECHANICAL DATA

<i>ID</i>	<i>Loading rate (m/s)</i>	<i>Force (N)</i>	<i>Deflection (mm)</i>	<i>Stiffness (N/mm)</i>	<i>Energy (J)</i>	<i>Pathology</i>
1	0.002	4464	9.1	790	18.88	Linear fracture—left temporal and parietal bones
2	0.002	5292	8.9	695	18.57	Linear fracture—orbital roof
3	0.002	5915	7.8	1143	14.07	Linear fracture—parietal, temporal, zygomatic bones
4	0.002	6182	15.4	487	44.72	Depressed fracture—inferior parietal, temporal bones
5	0.002	4642	14.1	467	36.28	Multiple depressed fracture—frontal bone
6	0.002	11898	16.6	1290	68.47	Circular fracture—lambdoid suture
7	7.2	14034	5.72	4798	31.46	Linear fracture—vertex to right orbit, frontal bone
8	7.1	13600	4.01	5867	23.51	Multiple fracture—frontal bone, LeFort III
9	7.6	13579	7.40	2540	40.00	Multiple fracture—through vertex, frontal, temporal bones
10	7.3	10009	9.74	2462	43.48	Circular fracture—superior to lambda
11	7.8	8809	3.44	4078	15.59	Multiple fracture—parietal bone, bilateral
12	8.0	11595	4.56	4394	14.06	Circular fracture—vertex region
Mean (1–6)		6399	12.0	812	33.5	
SE		(± 1134)	(± 1.6)	(± 139)	(± 8.5)	
Mean (7–12)		11938	5.8	4023	28.0	
SE		(± 885)	(± 1.0)	(± 541)	(± 5.1)	

BIOMECHANICS OF SKULL FRACTURE

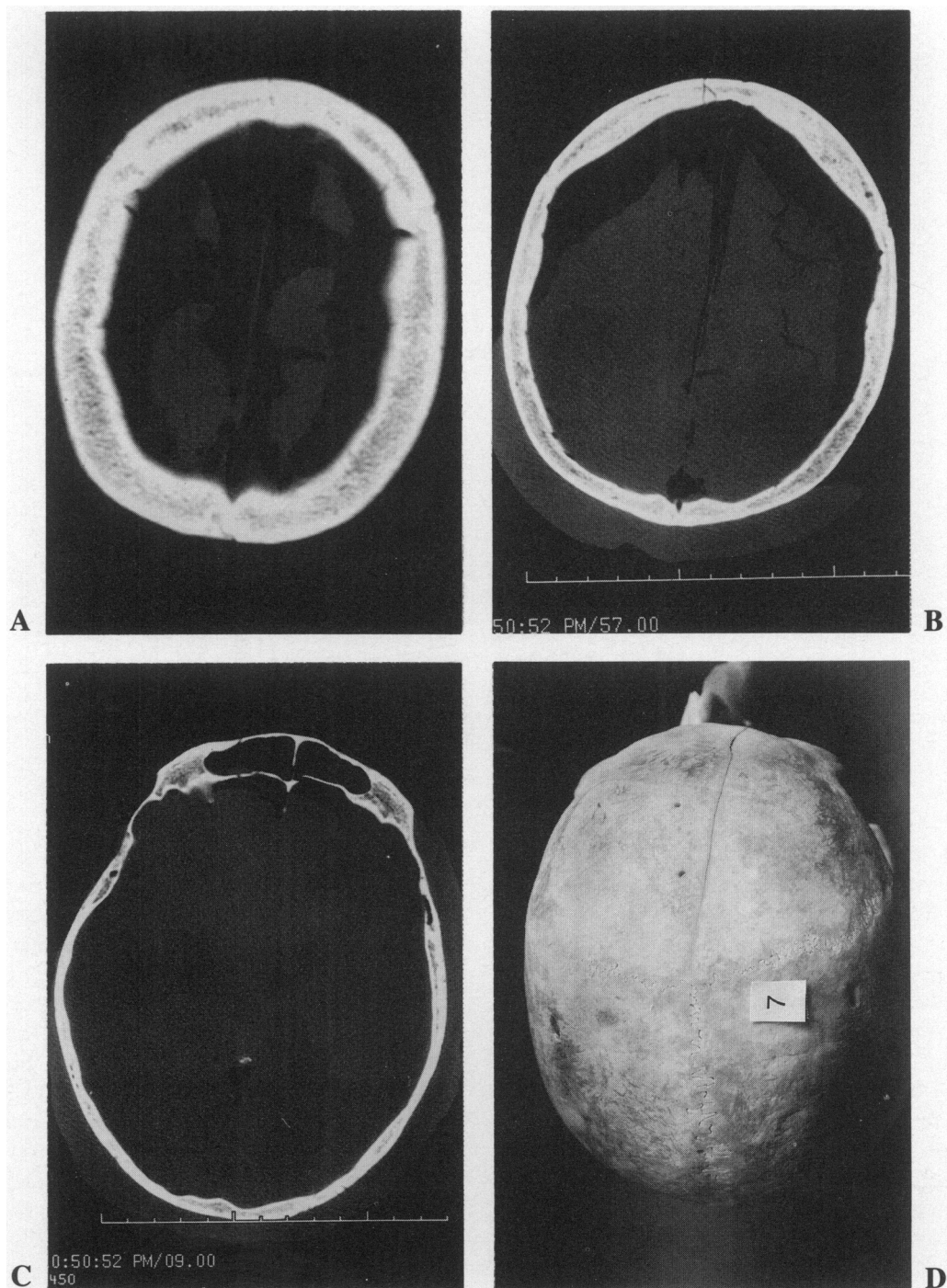


FIG. 4. Axial computed tomography images of specimen (#7) tested at an impact velocity of 7.2 m/s at the vertex. (A) Scan close to the impact site. (B) At 17 mm from image shown in (A). (C) At 65 mm from image shown in (A). Note the well-defined fracture of the calvarium in (B) and (C) compared to (A). Fracture of the frontal sinus is also seen in (C). (D) Top view of the defleshed specimen depicting the linear skull fracture, becoming more pronounced away from the vertex, the impact site.

mm. After reaching this level, continuing application of the insult resulted in an increase of the force before reaching failure. The structure demonstrated local yield phenomenon at the first peak force of 3.4 kN resulting in an

initial damage to the outer table of the calvarium, and at the ultimate force of 4.5 kN with a corresponding displacement of 9.1 mm, the inner table fractured reaching the load carrying capacity. Figure 5 shows the fractures

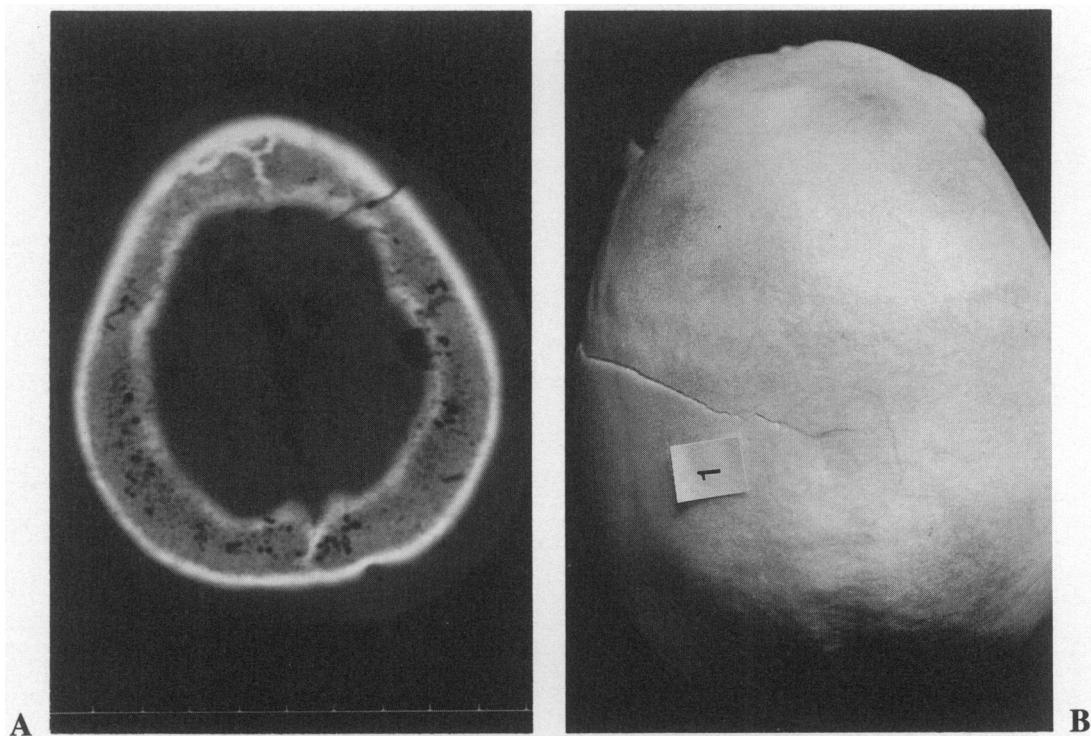


FIG. 5. (A) Axial computed tomography section of specimen #1 tested quasistatically at the vertex to failure. Note the fracture of both the inner and outer tables. (B) Top view of the defleshed skull depicting the linear fracture. The fracture is widened distal from the loading site. Note the area of indentation immediately surrounding the vertex indicating the area of contact.

of both the inner and outer tables. In other words, the biomechanical force–deflection response provided quantified data regarding the plausible fracture mechanism and forces of the calvarium. Similar micro failures or yielding phenomena were not apparent on the dynamic loading experiments. This is probably due to the high rate of onset that may have resulted in simultaneous fracture propagation. Techniques such as optical motion analysis and acoustic emission methods may be useful in exploring further the identification of the pathology.

Results of the present study in terms of the structural characterization compare favorably with earlier quasistatic tests conducted by McElhaney et al. (1972). In this previous investigation, fresh unembalmed human cadavers were positioned so that the head rested between two 150-mm-diameter steel plates. Static loading was applied and force–deflection curves were obtained for left to right and anteroposterior vectors. Stiffnesses, based on these curves at higher ranges of loading, ranged from 150 to 3500 N/mm. The force–deflection curves reported in this previous study compare well with our findings. The authors, however, did not discuss the pathological alterations, if any, sustained by the specimen. Consequently, a comparison of this earlier study with the fractures obtained in the present research is not possible. To the best

of our knowledge, the present investigation is the only study to provide the biomechanical force–deflection response and the ensuing pathology documented by X-ray, CT, and defleshing techniques, for intact human cadaver heads under external loading.

Considerable research has been conducted in the past to understand the mechanisms of injury to the human head; this includes skull fractures and brain trauma (Allsop, 1993; Becker and Povlishock, 1985; Cooper, 1982; Got et al., 1978; Goldsmith, 1972; Gurdjian, 1975; Gurdjian et al., 1961, 1958; Harris et al., 1981; Hodgson, 1967; Hodgson et al., 1970; Hodgson and Thomas, 1972; Jennett et al., 1977; Nahum et al., 1980, 1981; Nakamura et al., 1986; Newman, 1993; Odom, 1979; Ommaya, 1985; Ono et al., 1980; Sances et al., 1981; Sances and Yoganandan, 1986; Schneider and Nahum, 1972; Yoganandan et al., 1990). There is a plethora of clinical and epidemiological studies dealing with the various aspects of head injury including skull fracture, subdural and epidural hematomas, brain stem injury, diffuse axonal shearing, and the underlying clinical mechanism postulates. However, the biomechanical aspects of skull fracture have primarily relied on impact methods such as the drop technique or loading the specimen with an impactor of a specific geometry, such as circular or flat surfaces.

BIOMECHANICS OF SKULL FRACTURE

Studies on facial injuries are also available (Yoganandan et al., 1989, 1991). Routinely, the input impact energy and the acceleration at a predetermined location on the surface of the head have been reported in drop test experiments; similar data together with the impactor contact area are available in the latter type of experiments. These biomechanical data have enriched our understanding of the structural behavior and led to the present advancements. In the present study, force-deflection and other related properties of the skull under controlled and repeatable varying rates of load application with the associated pathology are obtained. Some preliminary data on the quasistatic response were reported (Yoganandan et al., 1994). This information is crucial for the development and validation of a mathematical model of the head. For example, the three-dimensional bony geometry of the specimen can be obtained from the CT scans, the exact boundary and loading conditions used in the experiment can be appropriately specified in the mathematical model, and the output experimental force-deflection characteristics can be used for the validation of the mathematical model. This procedure leads to the advancement of an experimentally validated three-dimensional finite element model of the human head that can be used to conduct parametric studies under real-world traumatic loading situations and predict injury. The present series of experiments provide an opportunity to accomplish these goals in a systematic fashion.

ACKNOWLEDGMENTS

This research was supported in part by the George Sniively Research Foundation, DOT NHTSA-93-Y-17028, PHS CDC Grants R49CCR-507370 and 703640, and the Department of Veterans Affairs Medical Research Service.

REFERENCES

- ALLSOP, D. (1993). Skull and facial bone trauma: Experimental aspects, in: *Accidental Injury, Biomechanics and Prevention*. A.M. Nahum and J.W. Melvin (eds.). Springer-Verlag: Berlin, pp. 247-267.
- BECKER, D.P., and POVLISHOCK, J.T. (eds.). (1985). *Central Nervous System Trauma Status Report*. NIH, NINCDS: Washington, DC.
- COOPER, P.R. (1982). *Head Injury*. Williams & Wilkins: Baltimore, MD.
- DIMASI, F., EPPINGER, R.H., GABLER, H.C., and MARCUS, J.H. (1991). Simulated head impacts with upper anterior structures using rigid and anatomic brain models. *Auto Traffic Safety* 20-31.
- EWING, C.L., THOMAS, D.J., SANCES, A., JR., and LARSON, S.J. (eds). (1983). *Impact Injury of the Head and Spine*. Charles C Thomas: Springfield, IL.
- GOLDSMITH, W. (1972). Biomechanics of head injury, in: *Biomechanics, Its Foundations and Objectives*. Y.C. Fung, N. Perrone, and M. Anliker (eds.). Prentice-Hall: Englewood Cliffs, NJ, pp. 585-634.
- GOT, C., PATEL, A., FAYON, A., TARRIERE, C., and WALFISCH, G. (1978). Results of experimental head impacts on cadavers: The various data obtained and their relations to some measured physical parameters. 22nd Stapp Car Crash Conf. 55-99.
- GURDJIAN, E.S. (1975). *Impact Head Injury, Mechanistic, Clinical and Preventative Correlations*. Charles C Thomas: Springfield, IL.
- GURDJIAN, E.S., and WEBSTER, J.E. (1958). *Head Injuries: Mechanisms, Diagnosis, and Management*. Little, Brown: Boston.
- GURDJIAN, E.S., LISSNER, H.R., EVANS, F.G., PATRICK, L.M., and HARDY, W.G. (1961). Intracranial pressure and acceleration accompanying head impacts in human cadavers. *Surg. Gynecol. Obstet.* 185-190.
- HARRIS, S.H., KALSBECK, W.D., and McLAURIN, R.L. (1981). The National Head and Spinal Cord Injury Survey: An overview of the study and selected findings relative to head injury, in: *Head and Neck Injury Criteria, A Consensus Workshop*. Washington, DC, pp. 6-10.
- HODGSON, V.R. (1967). Tolerance of the facial bones to impact. *Am. J. Anat.* 120, 113-122.
- HODGSON, V.R., and THOMAS, L.M. (1972). Comparison of head acceleration injury indices in cadaver skull fracture. 15th Stapp Car Crash Conf. 190-206.
- HODGSON, V.R., BRINN, J., THOMAS, L.M., and GREENBERG, S.W. (1970). Fracture behavior of the skull frontal bone against cylindrical surfaces. 14th Stapp Car Crash Conf. 341-355.
- JENNETT, B., TEASDALE, G., GALBRAITH, S., PICKARD, J., GRANT, H., BRAAKMAN, R., AVEZAAT, C., et al. (1977). Severe head injuries in three countries. *J. Neurol. Neurosurg. Psychiat.* 40, 291-298.
- McELHANEY, J.H., STALNAKER, R.L., and ROBERTS, V.L. (1972). Biomechanical aspects of head injury, in: *Human Impact Response*. W.F. King and H.J. Mertz (eds.). Plenum Press: New York, pp. 85-112.
- MELVIN, J.W., LIGHTHALL, J.W., and UENO, K. (1993). Brain injury biomechanics, in: *Accidental Injury, Biomechanics and Prevention*. A.M. Nahum and J.W. Melvin (eds.). Springer-Verlag: Berlin, pp. 268-291.
- NAHUM, A., WARD, C., RAASCH, E., ADAMS, S.,

- and SCHNEIDER, D. (1980). Experimental studies of side impact to the human head, 24th Stapp Car Crash Conf. 43–62.
- NAHUM, A., WARD, C., SCHNEIDER, D., RAASCH, E., and ADAMS, S. (1981). A study of impacts to the lateral protected and unprotected head. 25th Stapp Car Crash Conf. 241–270.
- NAKAMURA, N., SEKINO, H., MASUZAWA, H., MII, K., KIKUCHI, A., ONO, K., and KOBAYASHI, H. (1986). Experimental head injuries due to direct impact acceleration—head tolerance limit to impact, in: *Mechanisms of Head and Spine Trauma*. A. Sances, Jr., D.J. Thomas, C.L. Ewing, S.J. Larson, and F. Unterharnscheidt (eds.). Aloray Publishers: New York, pp. 219–235.
- NEWMAN, J.A. (1993). Biomechanics of head trauma: Head protection, in: *Accidental Injury, Biomechanics and Prevention*. A.M. Nahum and J.W. Melvin (eds.). Springer-Verlag, Berlin, pp. 292–310.
- ODOM, G.L. (1979). In, *Central Nervous System Trauma Research Status Report*. National Institute of Neurological and Communicative Disorders and Stroke, NIH, Public Health Service: Washington, DC.
- OMMAYA, A.K. (1985). Biomechanics of head injury: Experimental aspects, in: *The Biomechanics of Trauma*. A.M. Nahum and J.W. Melvin (eds.). Appleton-Century-Crofts: New York, pp. 245–269.
- ONO, K., KIKUCHI, A., NAKAMURA, M., KOBAYASHI, H., and NAKAMURA, N. (1980). Human head tolerance to sagittal impact reliable estimation deduced from experimental head injury using subhuman primates and human cadaver skulls. 24th Stapp Car Crash Conf. 101–160.
- SANCES, A., JR., and YOGANANDAN, N. (1986). Human head injury tolerance, in: *Mechanisms of Head and Spine Trauma*. A. Sances, Jr., D.J. Thomas, C.L. Ewing, S.J. Larson, and F. Unterharnscheidt (eds.). Aloray Publishers: New York, pp. 189–218.
- SANCES, A., JR., MYKLEBUST, J.B., LARSON, S.J., CUSICK, J.F., WEBER, R.C., and WALSH, P.R. (1981). Bioengineering analysis of head and spine injuries. *CRC Crit. Rev. Bioeng.* **5**, 79–122.
- SCHNEIDER, D.C., and NAHUM, A.M. (1972). Impact studies of facial bones and skull. 16th Stapp Car Crash Conf. 186–203.
- SNYDER, R.G. (1970). *Human Impact Tolerance*. Int. Automobile Safety Conf. Compendium, Society of Automotive Engineers: NY, Paper #700398, pp. 1375–1452.
- YOGANANDAN, N., PINTAR, F., SANCES, A., JR., et al. (1989). Steering wheel induced facial trauma. *SAE Transact.* **97**, 1104–1128.
- YOGANANDAN, N., HAFFNER, M., MAIMAN, D.J., et al. (1990). Epidemiology and injury biomechanics of motor vehicle related trauma to the human spine. *SAE Transact.* **98**, 1790–1807.
- YOGANANDAN, N., SANCES, A., JR., PINTAR, F.A., MAIMAN, D.J., HENNY, D., LARSON, S.J., and HAUGHTON, V. (1991). Traumatic facial injuries with steering wheel loading. *J. Trauma* **31**(5), 699–710.
- YOGANANDAN, N., SANCES, A., JR., PINTAR, F.A., et al. (1994). Biomechanical tolerance of the cranium. *SAE Paper* #941727.
- YOGANANDAN, N., CUSICK, J.F., PINTAR, F.A., DROESE, K., and VOO, L. (1995). An experimental technique to induce and quantify complex cyclic forces to the lumbar spine. *Neurosurgery* **36**(5), 956–964.

Address reprint requests to:
 Dr. Narayan Yoganandan
 Department of Neurosurgery
 MCW Clinic at FMLH
 Medical College of Wisconsin
 9200 West Wisconsin Avenue
 Milwaukee, WI 53226